Characterization of the microwave coplanar waveguide resonators designed for cQED architecture with Xmon qubits

G. Fedorov

September 9, 2016

Please find the most recent version of this report at GitHub

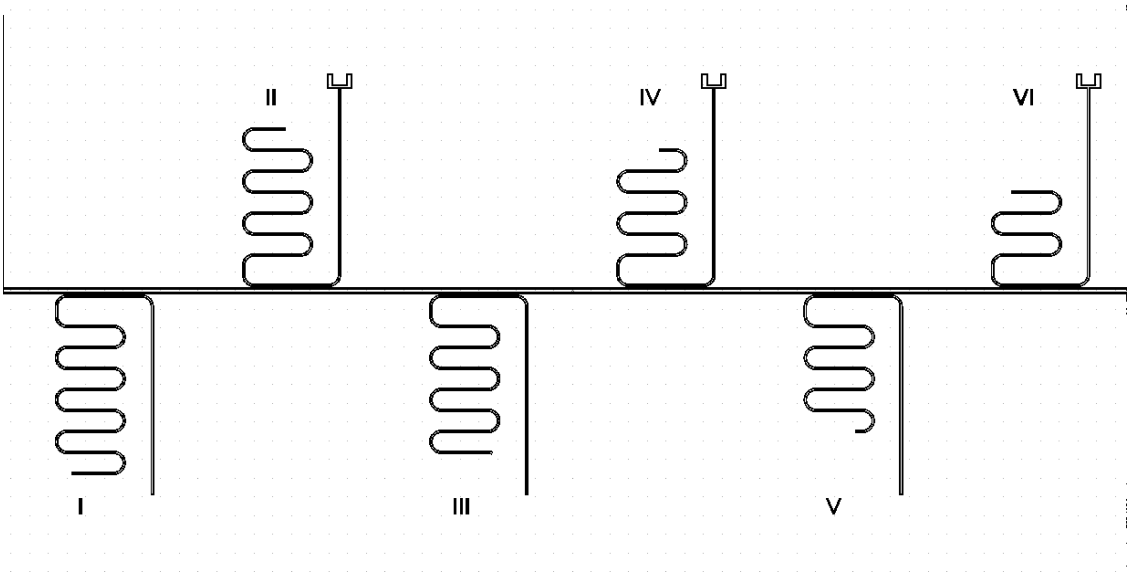

Contents

1 Nb CPW resonators: Q-factors and frequencies

The sample with niobium resonators (design shown under the title) was created in the cleanroom facility of the Laboratory of Superconducting Metamaterials. Using photolithography and then ion etching an approximately 30 nm Nb film on a Si/SiO_2 substrate was patterned and after that the chip was cut out with a saw. The sample was characterized using standard microwave methods firstly at MISIS and then at ISSP. Finally, the results were analysed using the fitting technique developed[1] by S. Probst et al.

The sample consists of a coplanar waveguide feed and six microwave $\lambda/4$ coplanar waveguide resonators capacitively coupled to it. All of the important geometrical and electrical parameters of the devices may be retrieved from the QR code displayed below the title of this document. The lengths of the resonators were calculated to yield resonance frequencies of 6, 6.2, 6.5, 7, 7.6, 8.6 GHz in correspondence with the numbering of the devices on the chip. The dielectric constant of the substrate ε_{Si} which determines the electrical length for the μ-wave travelling inside the resonator has been taken to be 11.9 during the calculation. The real value of the permittivity observed in the experiment then will be calculated based on the deviation of the measured resonance frequencies from the theoretical expectations.

Interesting parameters for the fabricated devices are the three quality factors, namely loaded Q_l, internal Q_i and external Q_e, and the resonance frequencies in dependence on power. To be more precise, in the context of cQED experiments the most important regime is when a resonator is populated with 1-10 photons on average, because otherwise it will dephase the coupled qubit.

1.1 General review of the resonances

A wide frequency scan of the sample using a vector network analyser is presented in Figure 1.1. Each of the resonators is forming a sharp dip in the transmission at the corresponding frequency which can be readily seen from the graph.

It can also be seen from the data that resonance frequencies are shifted approximately 80-160 MHz to the high frequency domain. This is summarized in Table 1. At this point it is worth noting that the frequency calculation correction method[2] that should be applied due to the presence of the "claw" coupler indeed allows to compensate it's phase shift – the resonance frequencies for "claw" devices deviate from theory not more than for the ones without the couplers.

The origin of the frequency shift is a different value of ε_{Si} in comparison with the value used during the calculation. Indeed, the permittivity of Si depends on its temperature,[3] and the right value that should have been used is $\varepsilon_{Si} \approx 11.45$ instead of $\varepsilon_{Si} \approx 11.9$ which gives a 1.79% correction to the observed frequencies. The residual errors appear to be random and should have come from the fabrication of the meandering part of the resonators.

The quality factors are at coarse consideration approximately equal to each other. The fine analysis with fitting will follow in the corresponding subsection.

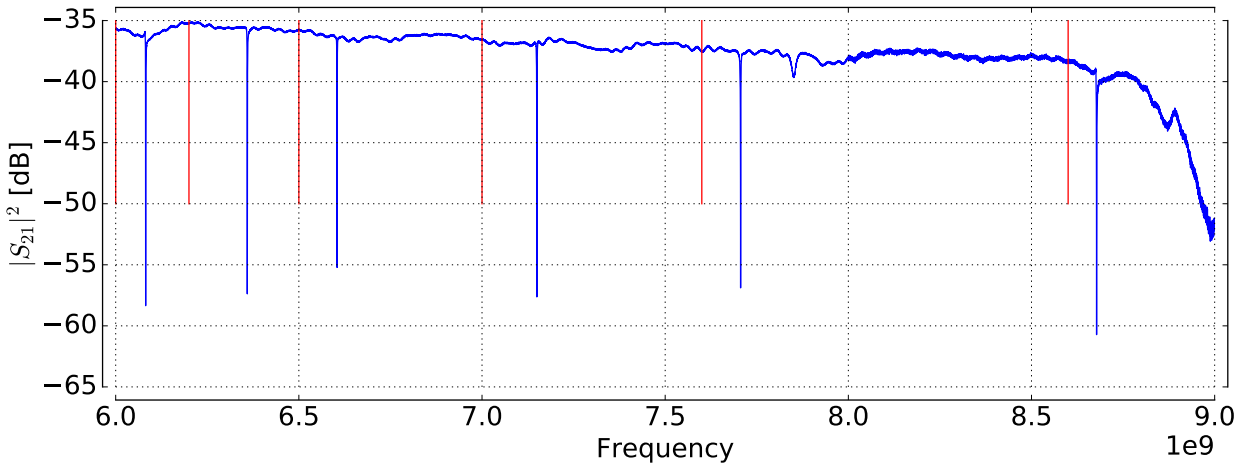

Figure 1.1: The frequency scan made at MISIS at 4K at high power. Six resonances are clearly visible, however each of them experienced an approximately 0.15 GHz shift up in frequency compared to the theoretical calculation.

	I	II	III	IV	V	VI
Expected [GHz]	6	6.2	6.5	7	7.6	8.6
Measured [GHz]	6.08	6.36	6.6	7.15	7.71	8.68
Difference [GHz]	0.08	0.16	0.1	0.15	0.11	0.08
Relative	1.4%	2.6%	1.6%	2.1%	1.4%	0.9%
Corrected	-0.4%	0.8%	-0.2%	0.3%	-0.4%	-0.9%

Table 1: Expected vs. measured resonance frequencies. Measured frequencies were extracted without fitting as local minima of S_{21} from Figure 1.1. Corrected row uses different ε_{Si} for theoretical values.

1.2 Subsequent cooldowns effect on the frequency

The first measurement which is displayed on Figure 1.1 was done at MISIS at a temperature of 4K and power too high to tell anything about so-called "one-photon" behaviour when the resonator is populated on average with no more than several photons. Therefore, a subsequent cooldown was required to measure the interesting qualities at low powers and temperatures. It was conducted two month later at ISSP in Chernogolovka at the temperature of 10 mK and a range of powers. After the second cooldown there was a noticeable and consistent change in resonance frequencies measured at high power, as shown in Figure 1.2. Each resonance shifted to the right approximately 1-5 MHz. This change may have been caused by a different temperature and, thus, different ε_{Si}.

Additionally the first resonator visually has a degraded Q-factor in comparison with the first experiment. It's possible that it was corrupted during the transportation; however, a detailed analysis with usage of microscopy may reveal a different origin.

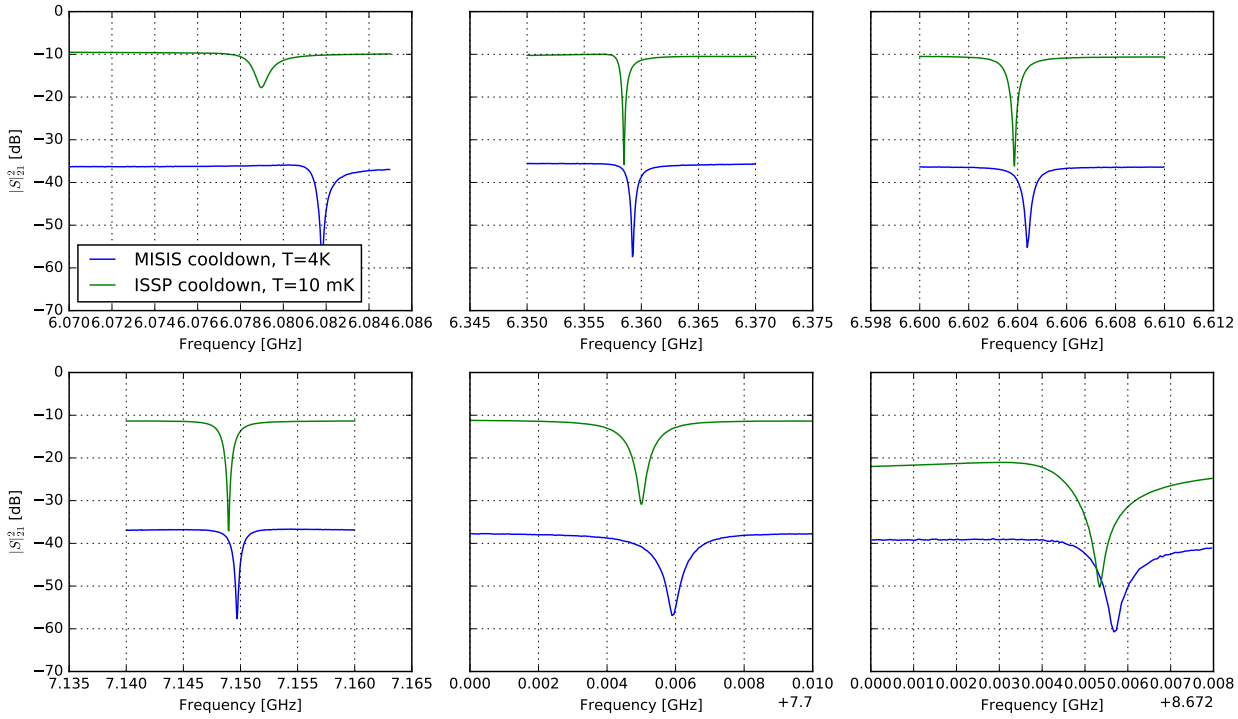

Figure 1.2: Changes in the resonators' frequencies after the second cooldown.

1.3 Fitting results

In this subsection the results obtained using the *circlefit* fitting method are presented. The raw data for the fitting was obtained using the standard qubit measurement architecture. Resonators where at the base plate of a dilution refrigerator at 10 mK, the attenuation was 60 dB to isolate room temperature noise. The signal then was amplified by a 30 dB HEMT and then by a 30 dB room temperature amplifier. Each peak from Figure 1.1 was enlarged and scanned with finer resolution and averaged to reduce noise (more averages on low and less on high powers). Then for each power the complex S_{21} data for each scan area around a resonance was recorded. In overall, such measurement was found to take 2-3 hours which is a modest time for experiments with cQED.

After all of the data had been obtained, the fitting procedure has been applied for every scan at each power. The full fitting process is described in depth in the original publication.[1] In practice, the whole algorithm is encapsulated in several function calls of the library called *resonator tools* that the authors have kindly provided via GitHub.

It is well-known[4] that for superconducting microwave resonators the internal quality factor experiences an increase in value when probed with higher power. This effect is believed to occur due to the presence of two-level defects or two-level systems (TLS) with a dipole moment in the areas of high electric fields which resonator creates. As long as TLSs have same frequency as the measured resonator and coupled strong enough, they will drain excitations from the resonator. However, TLSs can only accommodate only one photon at a time; thus, at high probe powers they saturate and do no more participate in resonator relaxation.

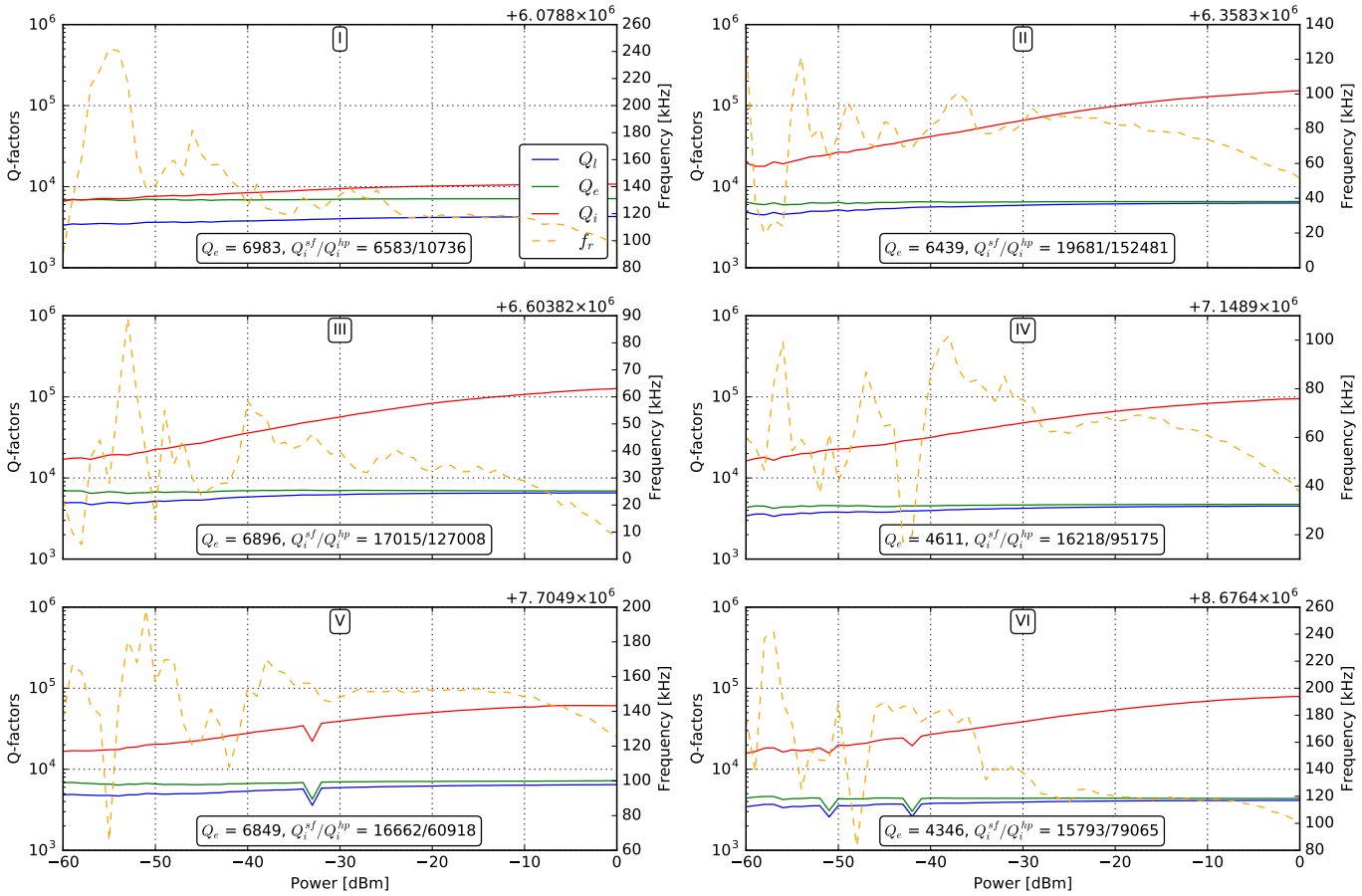

Figure 1.3: Various quality factors and frequencies in dependence on radiation power. Single photon limit is near -60 dBm on the VNA summed with 60 dB of attenuation, saturation limit near 0 dBm on the VNA. Standard behaviour consisting of a sigmoid-shaped increase of Q_i with incident power: marginal values are specified as Q^{sf} and Q^{hp}. Sudden fractures on the Q-factor lines are due to the fitting errors.

Therefore, the increase of the internal Q-factor is observed when the resonator is driven with strong microwave fields.

This is exactly what was observed while measuring the resonators at different probe powers. The fitting results are presented in Figure 1.3. From the first glance an expected dependence of Q_i on power is observed. Also, despite the fact the absolute values of Q_i^{hp} at high powers are very different for each resonator, at single-photon level all of the devices demonstrate similar Q_i^{sf} around 16500 except for the first resonator which for some reason has a significantly lower Q-factor than the others (this may be due to a shorting present somewhere inside it's waveguide). This demonstrates that defect distribution over the sample is more or less uniform and does not come from the post-processing like acetone washing or sawing.

The external quality factors are close to the theoretical expectations of approximately 7000 except for the devices IV and VI, where these values dropped to around 4000. The reasons for these deviations are unclear, because Q_e is determined only by the geometry of

the resonators and the only geometrical difference between the devices is the length of the meandering part. In general, the four main contributions in Q_e for this kind of resonators are the distance x between the hotwires of the feedline and a resonator, the coupling point distance from its open end, the length of the coupling segment parallel to the feedline and the overall area of the resonator's central wire. For the devices IV and VI it is difficult to find an explanation using the stated four parameters. Errors in photolithography are also not probable.

2 Bad Al CPW resonators: Q-factors and frequencies

The aluminium resonators sample was fabricated in the cleanroom facility at MIPT using photolithography and a lift-off procedure. They were then analysed with an approach similar to the one applied to the Nb sample. The design was identical to the design used for the fabrication of the previous sample. Unfortunately during the photolithography all of the central wires both for the resonators and the feedline experienced 10-20% broadening and during the lift-off some pieces of the ground plane near devices I and II were torn off. The sample was, nevertheless, measured, and the results studied.

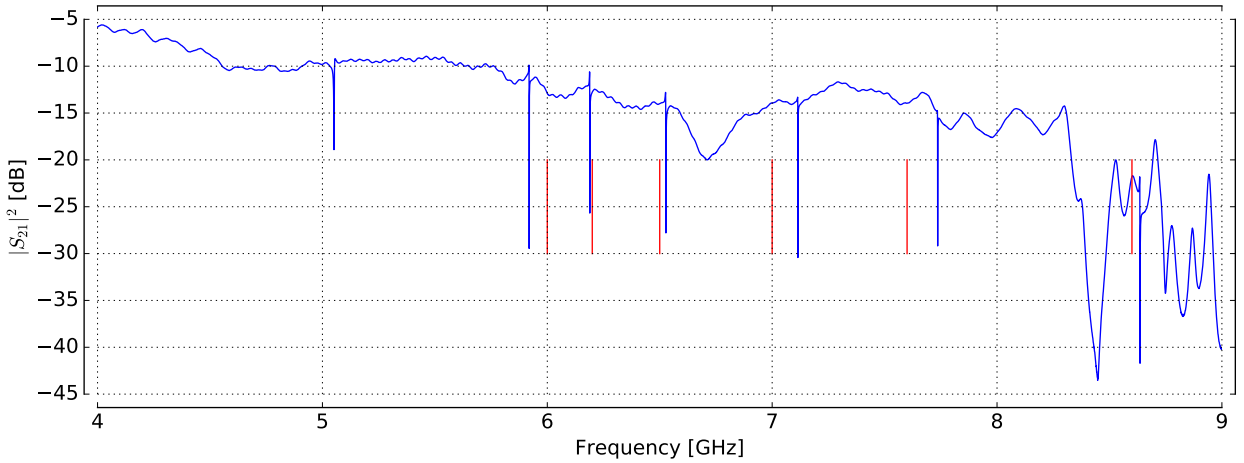

Figure 2.1: The frequency scan made at ISSP at 10 mK at high power. Vertical red lines show expected theoretical frequencies. Six resonances are clearly visible; however, a seventh one at approximately 5 GHz is also apparent.

2.1 General review of the resonances

Same as in the previous section the wide frequency scan of the sample is presented in Figure 2.1. One can notice that the frequencies of the resonances are shifted both to the left and to the right from the theoretical values. This is summarized in Table 2.

Despite the presence of both positive and negative deviations there is an upward trend of the relative shifts, possibly caused by a systematic error of the photolithograph. The errors thus may be due to the inaccurate fabrication. The correction procedure from the

	I	II	III	IV	V	VI
Expected [GHz]	6	6.2	6.5	7	7.6	8.6
Measured [GHz]	5.919	6.189	6.527	7.115	7.736	8.63
Difference [GHz]	-0.081	-0.011	0.027	0.115	0.136	0.03
Relative	-1.35%	-0.18%	0.42%	1.64%	1.79%	0.35%
Corrected	-3.05%	-1.88%	-1.28%	-0.06%	0.09%	-1.35 %

Table 2: Expected vs. measured resonance frequencies. Measured frequencies were extracted without fitting as local minima of S_{21} from Figure 2.1. Corrected row uses different ε_{Si} for theoretical values.

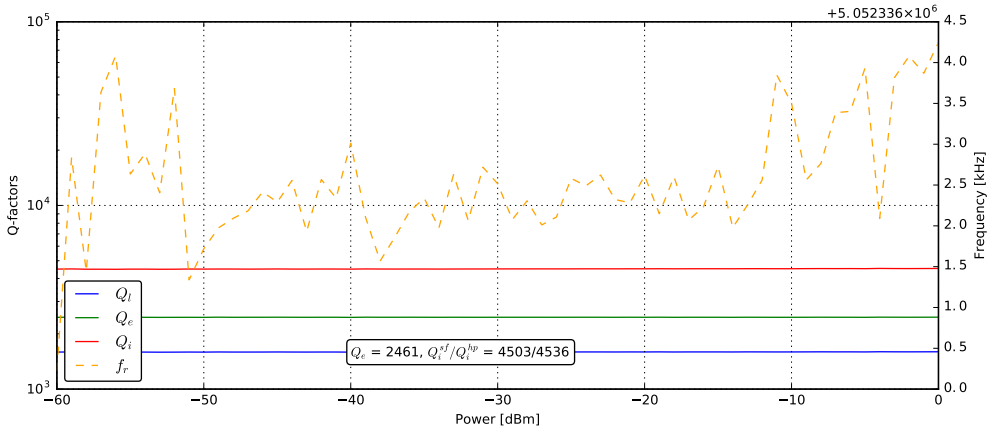

Figure 2.2: Spurious resonator frequency and quality factors in dependence on power.

previous section does not cure the values. It's not possible to extract the real ε_{Si} from the measurement data because the errors are not comparable throughout the resonators.

Also one can see an additional resonance in the vicinity of 5 GHz. It is believed to be spurious. It can't be a multiple mode of some resonator of lower frequency otherwise more modes would be visible on the graph in the area of higher frequencies. It can't be produced by any of the resonators because each of them is too short for that frequency. It is possible that this resonance had a second mode at 10 GHz, which would mean is as an effective $\lambda/2$ waveguide; however, this was not studied. All in all, there were different defects on the sample metallization so it should have been on of them.

Despite above said this resonance was also recorded and fitted, see Figure 2.2. It has demonstrated low internal quality factor of 4500 and external of 2500 which does not compare to any of the resonators assumed to be real.

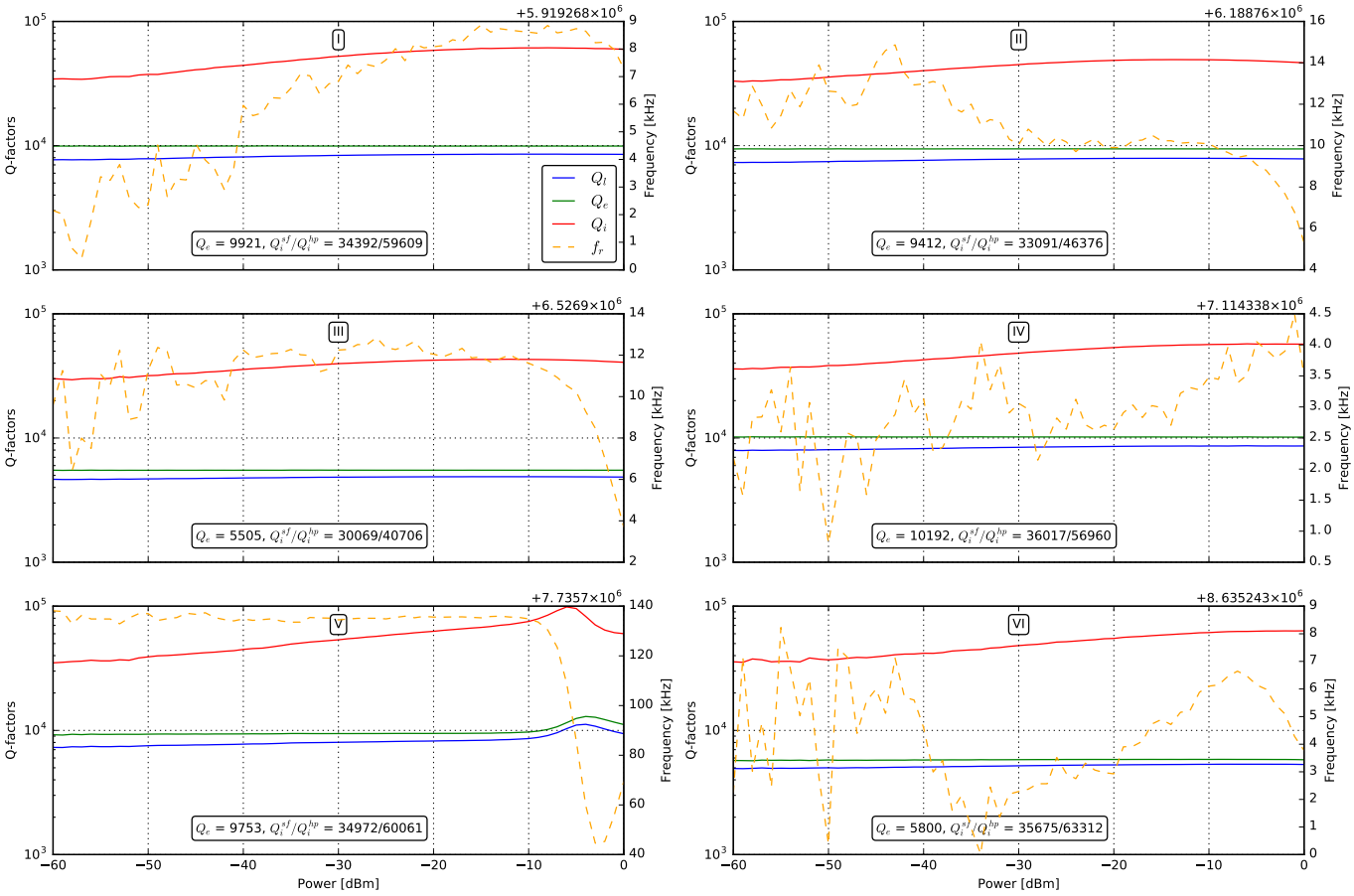

Figure 2.3: Various quality factors and frequencies in dependence on radiation power. Single photon limit is near -60 dBm on the VNA summed with 60 dB of attenuation, saturation limit near 0 dBm on the VNA. All devices show standard behaviour except for the V$^{\text{th}}$ which has an eccentric hump at high powers due to a fitting error or some different unknown reason.

2.2 Fitting results

Same as in the previous section the scan of the interesting properties over power is presented in Figure 2.3. Immediately we can see that the characteristics of the resonators are in deviation from their Nb brothers'.

Internal quality factors at high power are all significantly lower for this sample, which is likely to be caused by geometrical defects and inhomogeneity of Al film in the area of high currents. However, the single-photon Q_is are approximately two times the corresponding values on Nb. This shows immediately that Al is much cleaner than Nb and thus more suitable for superconducting qubits experiments.

The external quality factors Q_e are noticeably higher than on the Nb sample which is at the first glance surprising because due to the broadening of the central wires the coupling capacity should have increased and the Q_e dropped. However, a narrower gap in the coplanar waveguide leads to better localization of the EM field thus reducing the crosstalk. In this design the latter effect must have overcome the former and increased Q_es. Interestingly devices III and VI now have deviating external quality factors, not IV and VI as for the Nb sample. Reasons still unclear.

3 Second Al sample

3.1 General review of the resonances

Measured on April 22 2016.

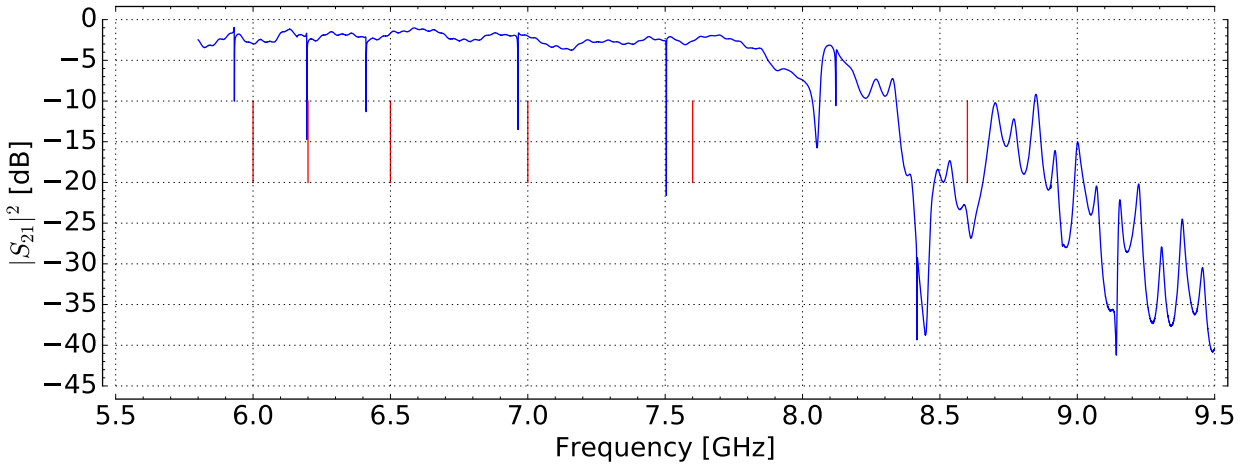

Figure 3.1: Frequency sweep of the second Al sample made at MIPT. It can be seen that five lower resonances correspond clearly to the expected resonator frequencies; however, there's nothing near the 6^{th} theoretical position. There are also three spurious resonances above 8 GHz which have low Q-factors and cannot be fit correctly.

3.2 Fitting results

Quality factors and frequencies of the lowest six resonances.

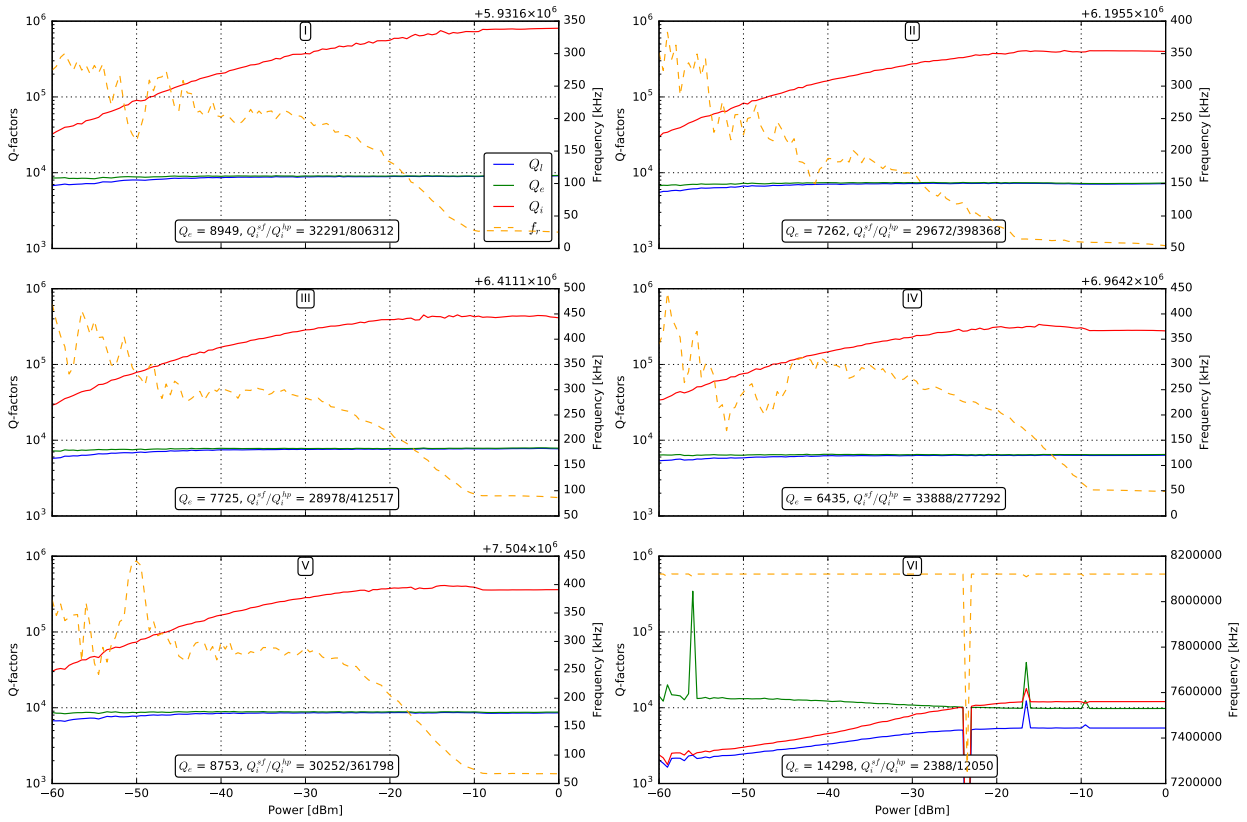

Figure 3.2: Fitting results for the six lowest resonances. The bottom right figure thus corresponds to one of the spurious resonances. The fitting errors and the deviation of the Q-factors behaviour compared to the other five resonances are visible. The other two spurious resonances demonstrated even worse results.

4 NbN 300 nm with changing gap sample

This sample was created in MISIS and measured on April 29$^{\text{th}}$ 2016. The design was different this time. Just as before, six resonators were coupled to the feedline; however, the coplanar width for each of them increased with resonator's index number. This change was made with an intent to check the dependence of Q_i on the electric field strength inside the coplanar gap.

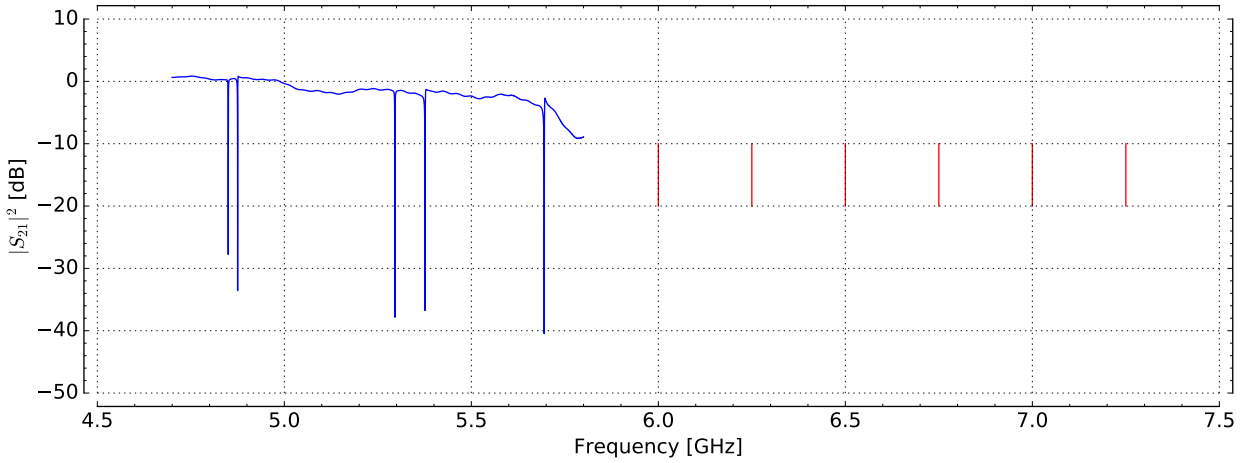

Figure 4.1: Frequency scan of the resonances on the NbN chip. Only five resonances were observed. Clearly, the frequencies are lower than expected from the geometrical length indicating that α is still noticeable, even at this film thickness.

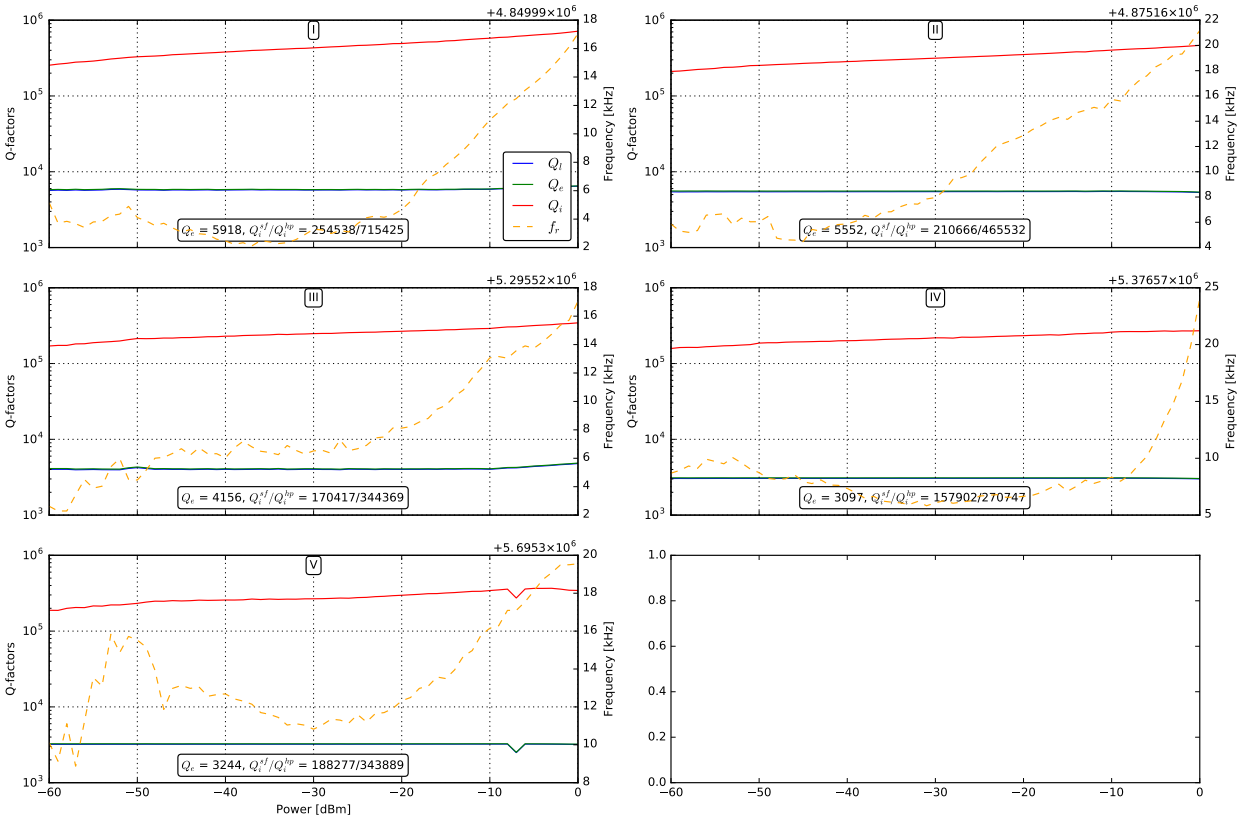

Figure 4.2: Fitting results. High internal quality factors can be noticed at all power levels. Both the external and internal Q-factors show an inverted dependence on the gap width. They are decreasing while from the theoretical model they should have been increasing.

4.1 General review of the resonances

4.2 Fitting results

5 Third Al sample (Res Al MIPT 1)

Third aluminium sample was also fabricated at MIPT and measured on June 26$^{\text{th}}$ 2016. It consists of two 4x8mm designs, one standard and one with varied coplanar gap width. Below results for the standard design are presented.

5.1 General review of the resonances

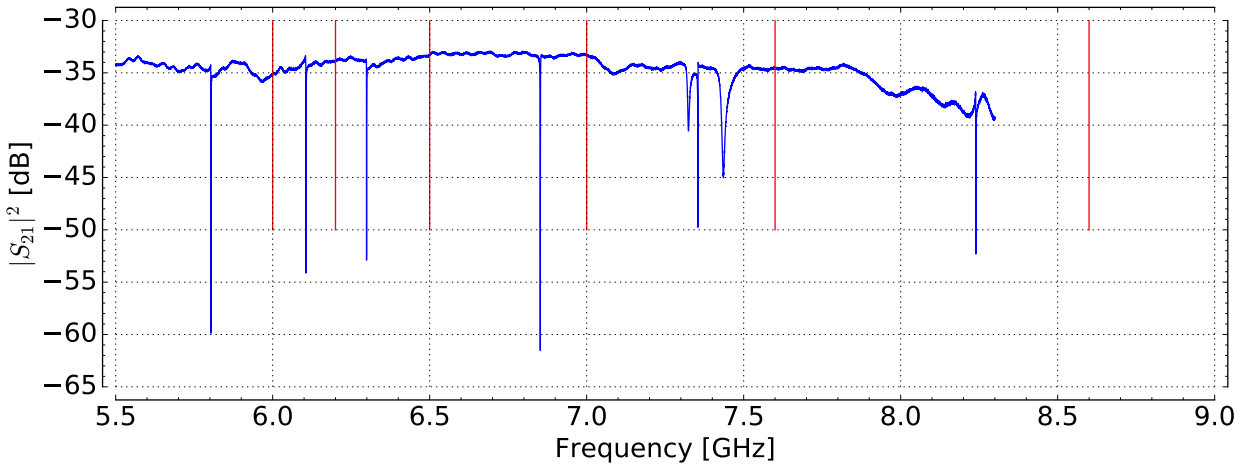

Figure 5.1: Frequency scan of the third Al sample. All six resonators are visible; though, there are two additional spurious low-Q resonances around the 5$^{\text{th}}$ one. The resonances are shifted down non-uniformly from their theoretical positions.

	I	II	III	IV	V	VI
Expected [GHz]	6	6.2	6.5	7	7.6	8.6
Measured [GHz]	5.8	6.1	6.3	6.85	7.35	8.24
Difference [GHz]	-0.2	-0.09	-0.2	-0.15	-0.25	-0.36
Relative	-3.39%	-1.54%	-3.19%	-2.16%	-3.34%	-4.38%

Table 3: Expected vs. measured resonance frequencies. Measured frequencies were extracted without fitting as local minima of S_{21} from Figure 5.1.

General view of the sample response can be seen on Figure 5.1. Eight resonances are visible, two of which are spurious having significantly lower Q-factors than others. Other six can be identified as resonators responses. It can be seen that the frequencies of the resonators

are lower than expected, and the shifts are not linear with respect to frequency, see Table 4. Frequency errors are also larger than in the previous experiments with aluminium samples.

5.2 Fitting results

Frequencies and quality factors were extracted as usual for different powers and are presented in Figure 5.2. Low-power Q-factors are ≈40% higher than for the previous aluminium samples. High-power Q's, however, are lower than for the second sample.

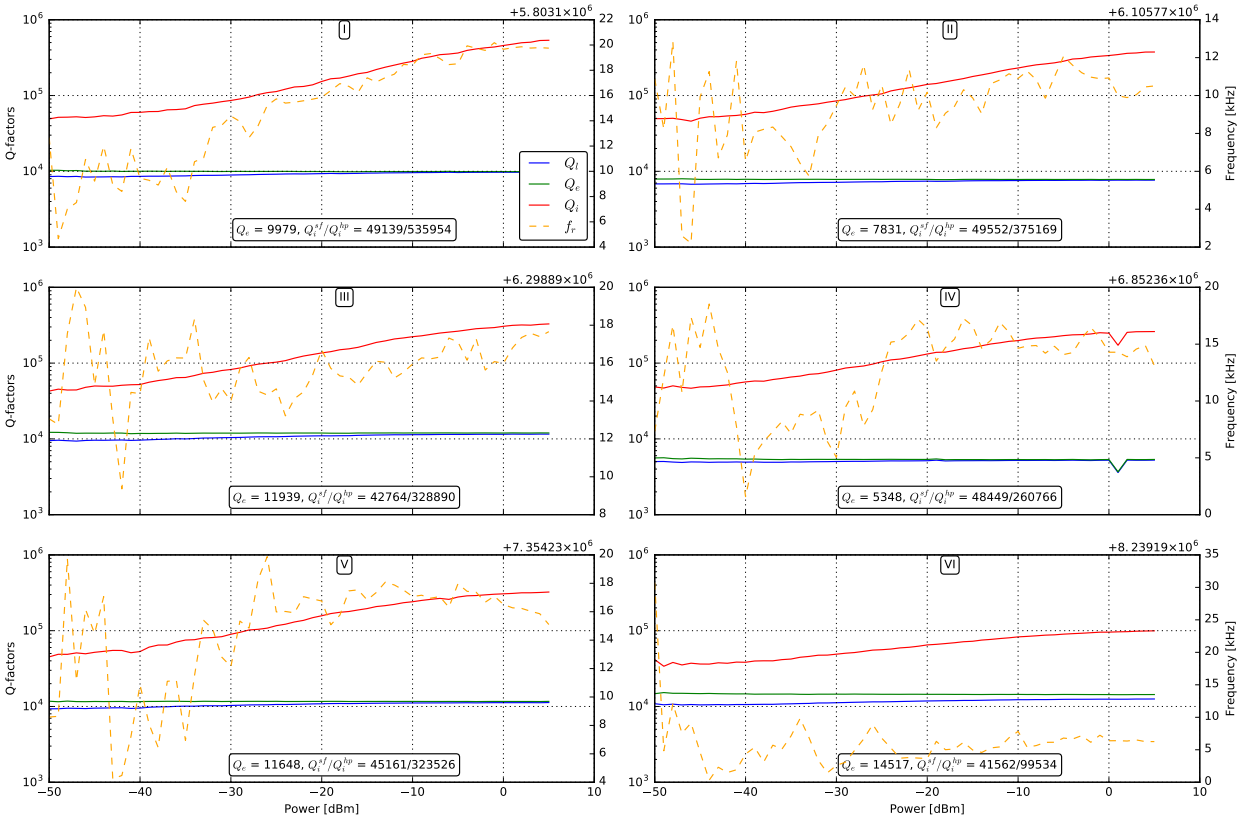

Figure 5.2: Fitting results for the third Al sample. All resonators demonstrate consistent low-power internal Q-factors around $4.5{\cdot}10^4$ and less consistent high-power Q-factors from $1{\cdot}10^5$ to $5{\cdot}10^5$.

6 Fourth Al sample (Res Al MIPT 2

Fourth aluminium sample was fabricated at MIPT by I. Khrapach and firstly measured on August 9, 2016. It is significantly different from the previous samples and consists of a single design presented in MISSING PICTURE FOR THE FIGURE. The fabrication method was also different for this sample, for it was made with two layers of Al, separated by a thin oxide layer.

In this section the data for two subsequent cooldowns is included due to the fact that in the first run not all necessary conditions for the correct determination of the quality factors were satisfied.

The first measurement of this sample was conducted without magnetic shielding. The temperature of the refrigerator was elevated at a value high above single-photon level (near 200 mK) in the beginning of the power scanning experiment but then dropped abruptly to 20 mK. It's unknown whether the measurement has been finished by that time, and thus it should be repeated because the temperature influences the internal Q-factors directly. Yet, the data from this unfortunate run is presented below.

At the same time, we present additionally the results for the repeated and refined measurement of this sample that was done on August 15, 2016, at the base temperature of 20 mK and with magnetic shielding.

6.1 General review of the resonances

No significant difference was observed between the general transmission pictures for these two runs, as can be seen from Figure 6.1 and Figure 6.2.

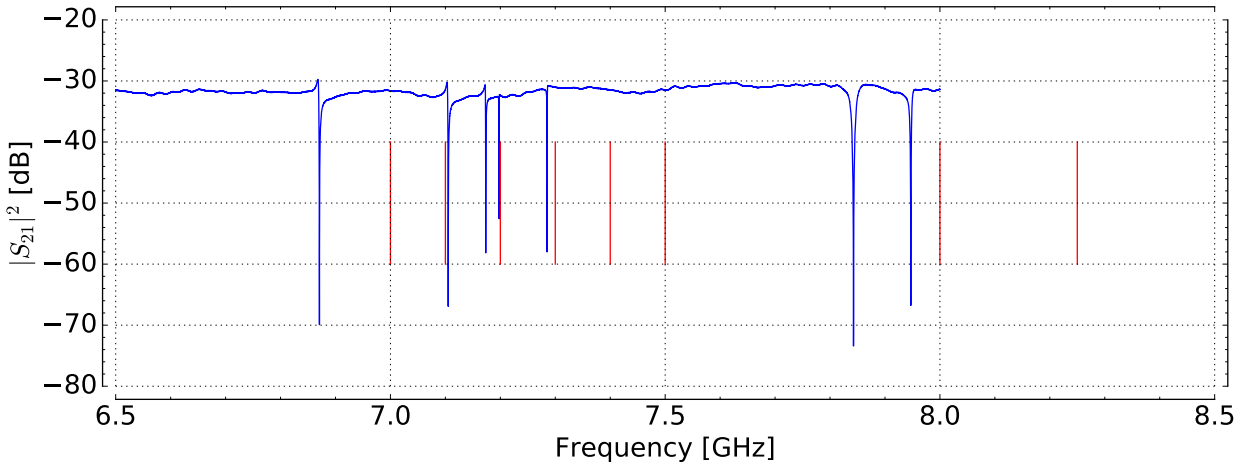

Figure 6.1: Frequency scan of the fourth Al sample. Five of the six lower-frequency resonances are visible, and both two higher-frequency ones from two test resonators. All resonances are shifted down non-uniformly from their theoretical positions.

All resonances have incorrect frequencies which also can be clearly seen from the figures. The shift is different for each of the resonators, and the differences show no systematic dependence on resonances' frequencies. Thus, these errors can't be attributed to the incorrect estimation of the substrate epsilon, as in the case with NbN samples.

6.2 Fitting results

In Figure 6.3 the fitting results are presented. It can be seen from the magnitude of the differences in the low-quality Q-factors that the first measurement was indeed at elevated

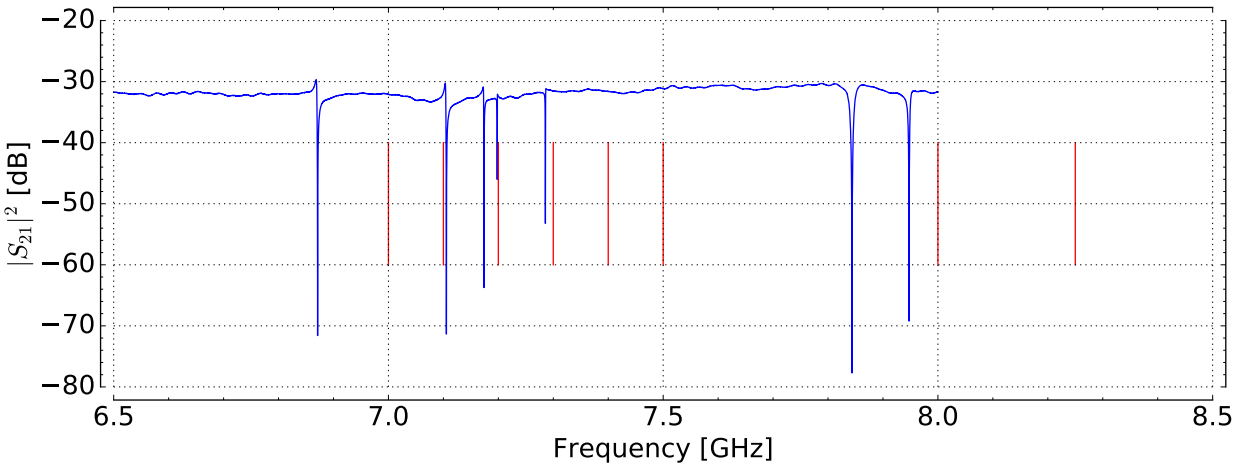

Figure 6.2: Same scan from the repeated measurement. All the features reproduce themselves.

	I	II	III	IV	V	VI	VII	VIII
Expected [GHz]	7	7.1	7.2	7.3	7.4	7.5	8	8.25
Measured [GHz]	6.87	–	7.11	7.17	7.2	7.29	7.84	7.95
Difference [GHz]	-0.13	–	-0.09	-0.13	-0.2	-0.21	-0.16	-0.3
Relative	-1.86 %	–	-1.25%	-1.78%	-2.7 %	-2.8 %	-2.00 %	-3.64 %

Table 4: Expected vs. measured resonance frequencies. Measured frequencies were extracted without fitting as local minima of S_{21} from Figure 6.2.

temperature (at least while lowest two-three resonators were measured); however, in overall, the results are pretty the same, indicating that the temperature was not too high and the magnetic shield didn't have a lot of influence in the first run.

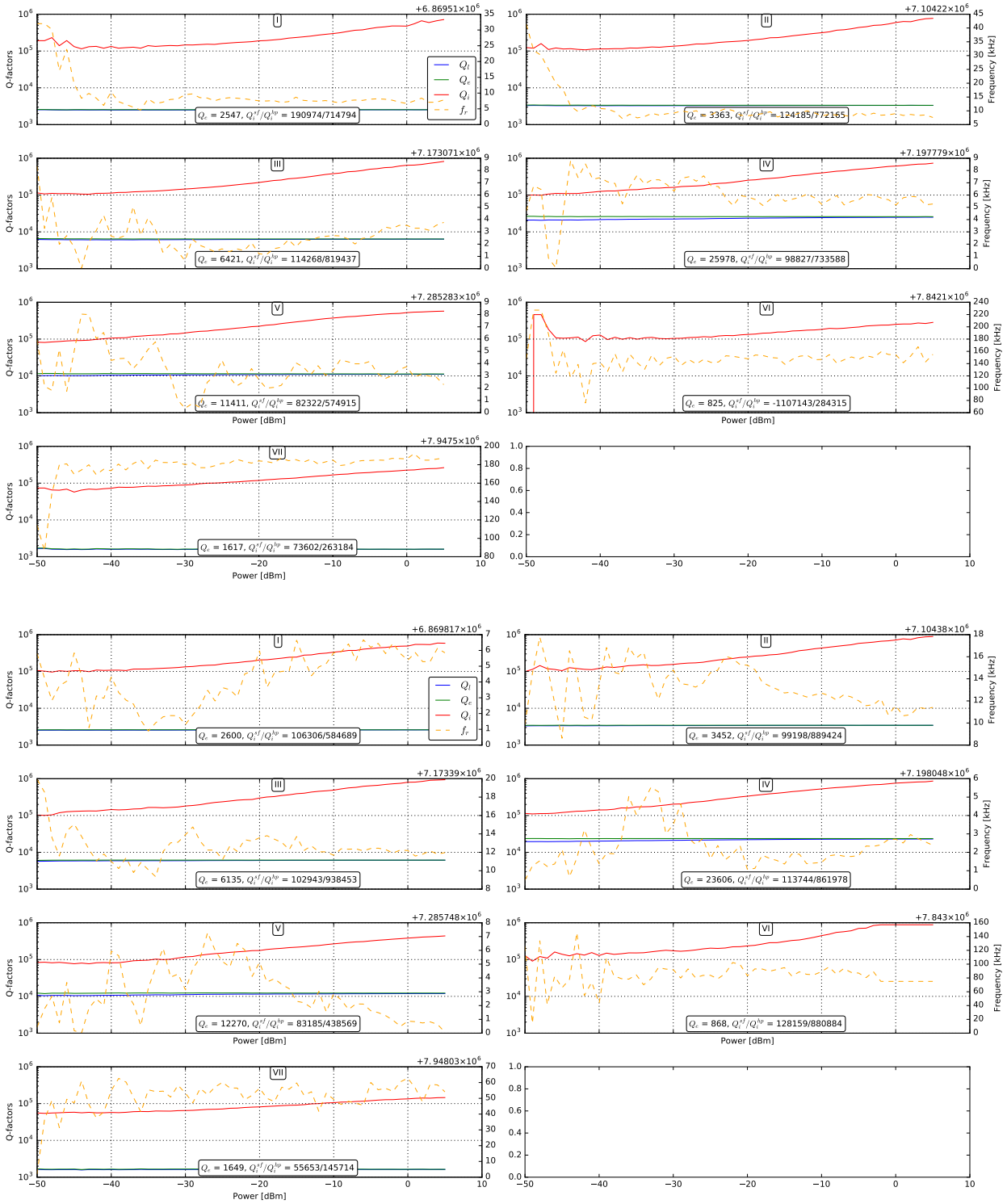

Figure 6.3: (Upper) Fitting results for the fourth Al sample, first run. All resonators demonstrate consistent high-power internal Q-factors around 5-7·10^5 and less consistent low-power Q-factors from 7·10^4 to 2·10^5. **(Lower)** Same plot with the data from the second run. Q-factors and curves in overall became more consistent.

7 Fifth Al sample (Res Al BMSTU 1)

7.1 General review of the resonances

A modified design with 12 resonators was fabricated at BMSTU and measured on August 26, 2016. The chip design is presented in Figure 7.1. It consists of three groups of devices, each consists of resonators with same theoretical external Q-factor. It is determined by the distance between the resonator and the feedline x. For the groups from the left to the right $x = 5, 10, 15$ μm, correspondingly.

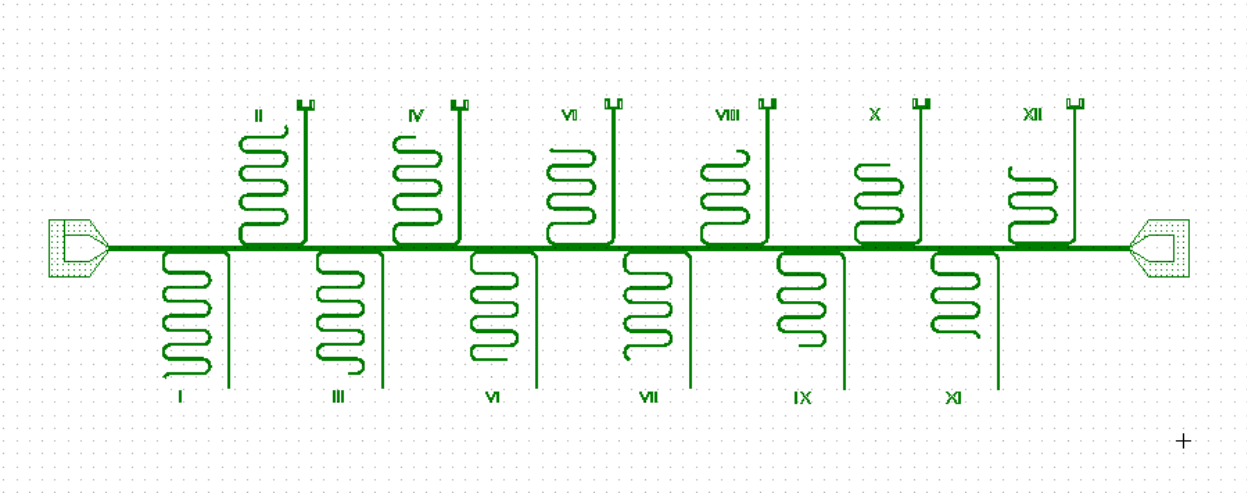

Figure 7.1: Sample design. Twelve resonators are divided into three groups with different coupling (can't bee seen due to the resolution).

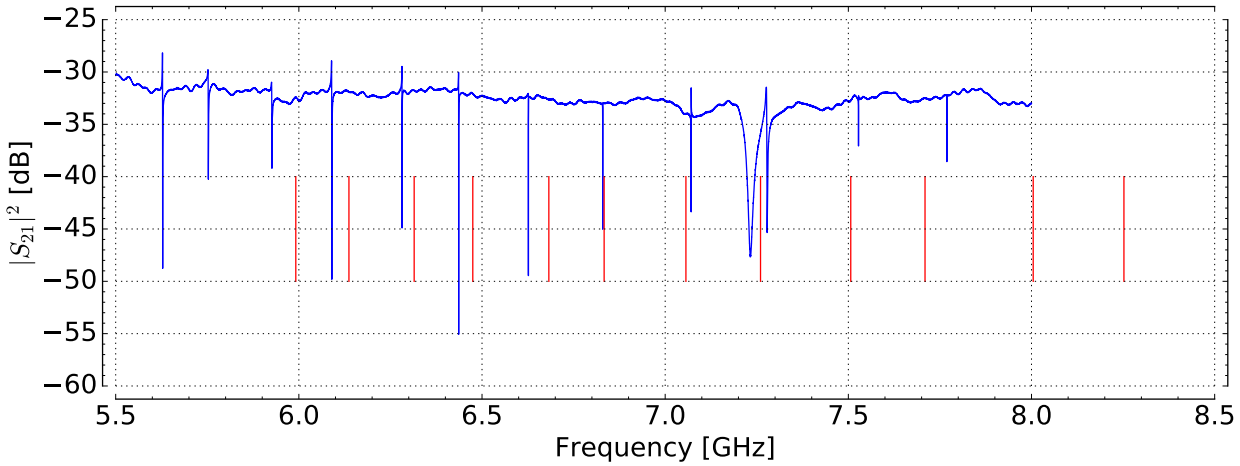

Figure 7.2: The frequency scan made at ISSP at 20 mK at high power. Twelve resonances are clearly visible; additionally, there's a low-Q parasitic one at approximately 7.25 GHz.

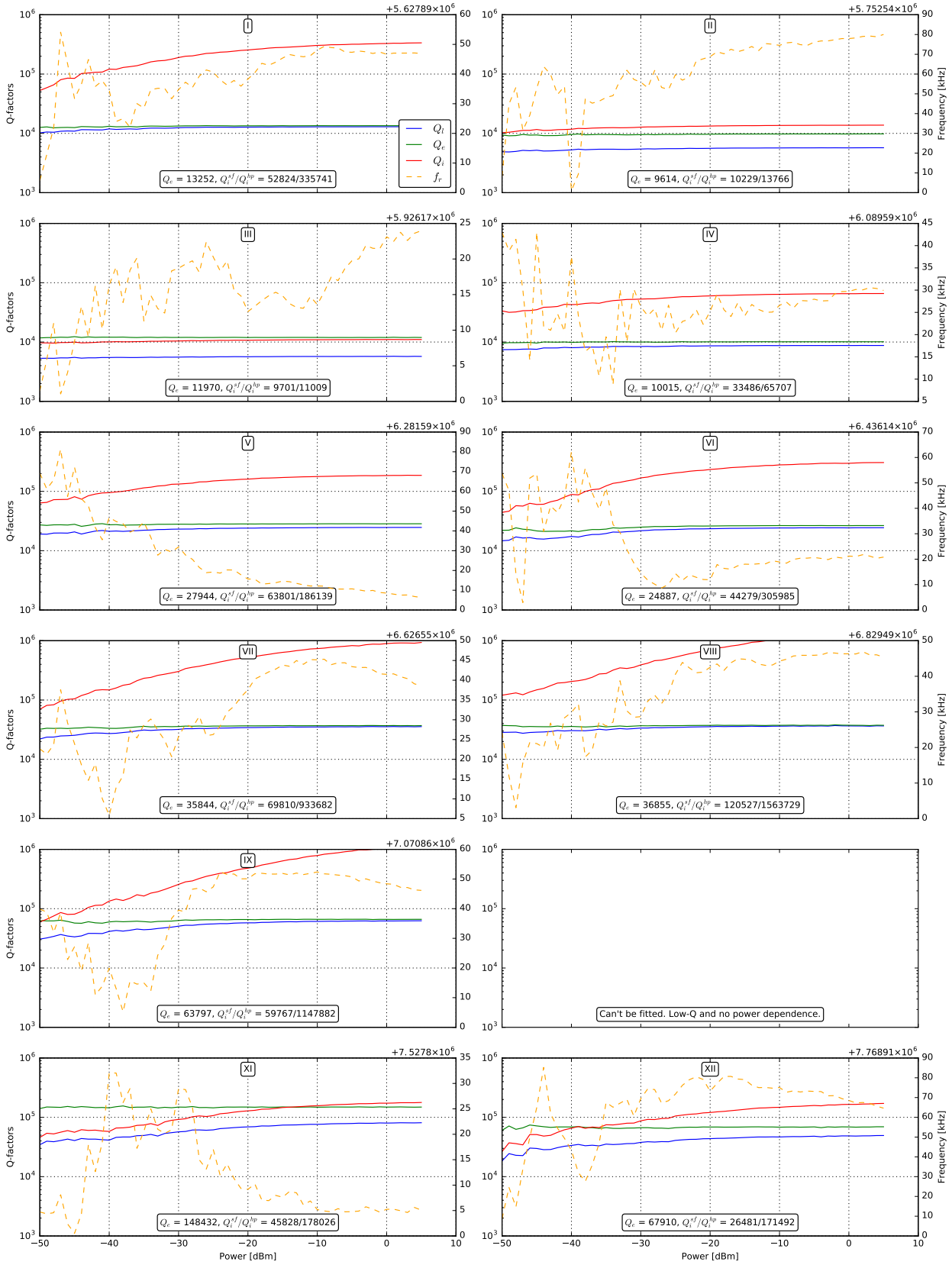

Figure 7.3: Fitting results for the fifth Al sample. Clearly, the three groups can be distinguished by the Q_e's they have. The internal low-power Q-factors span from 10^4 to 10^5, and all curves seem not to reach saturation at low powers. High power Q-factors span from 10^4 to $7 \cdot 10^5$.

7.2 Fitting results

The results of the fitting are presented in Figure 7.3. First feature to be noted is that all fitting curves don't reach saturation at low powers in contrast to the previous experiments with the same microwave setup. This means that the low-power Q-factors specified in the boxes under the figures are not actually single-photon and only give an upper bound on the Q_i's. The second feature is that the internal quality factors vary strongly among the devices. Even if resonators II, III and IV are excluded from the sample as clearly failed, still we will have a spread from 26k to 100k for the low-power Q_i's and from 170k to 1kk for the high-power ones.

8 Nb strongly etched on high-res Si (Res Nb MISIS 6) !GET FILM DEPOSITION PARAMETERS

This sample was fabricated at MISIS where the 110 nm Nb film was deposited by sputtering onto a strongly Ar-cleaned high-resistivity Si substrate and then etched through a photo-mask with SF_6. It was then measured on September 3, 2016.

8.1 General review of the resonances

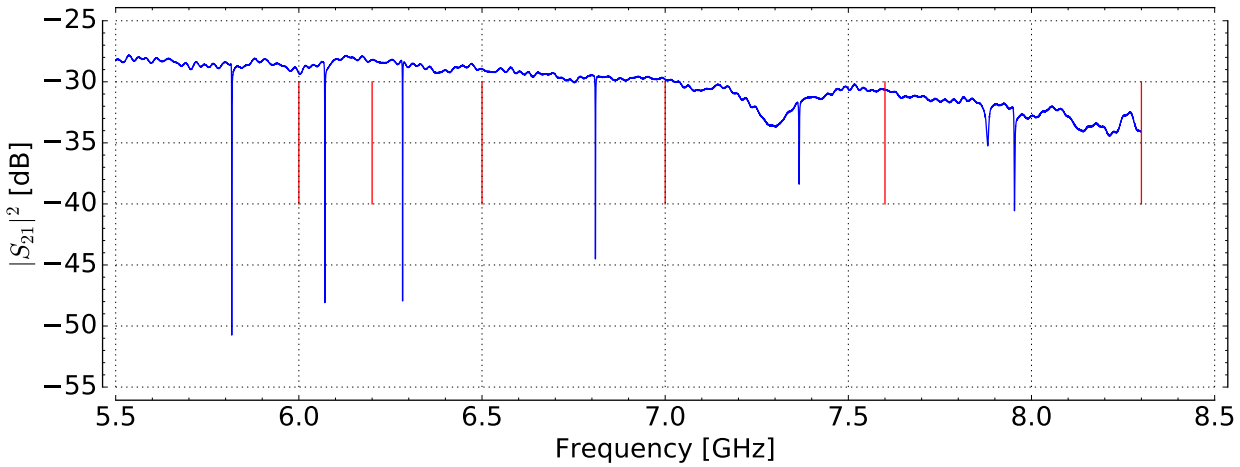

Figure 8.1: The frequency scan made at ISSP at 15 mK at high power. Six deep resonances and one shallow (presumably spurious) resonance are visible. Here green dashed lines show frequencies expected from length, red lines mark more accurate expectations considering non-zero coupling capacitances. Still, even with this correction, the frequency errors are significant.

8.2 Fitting results

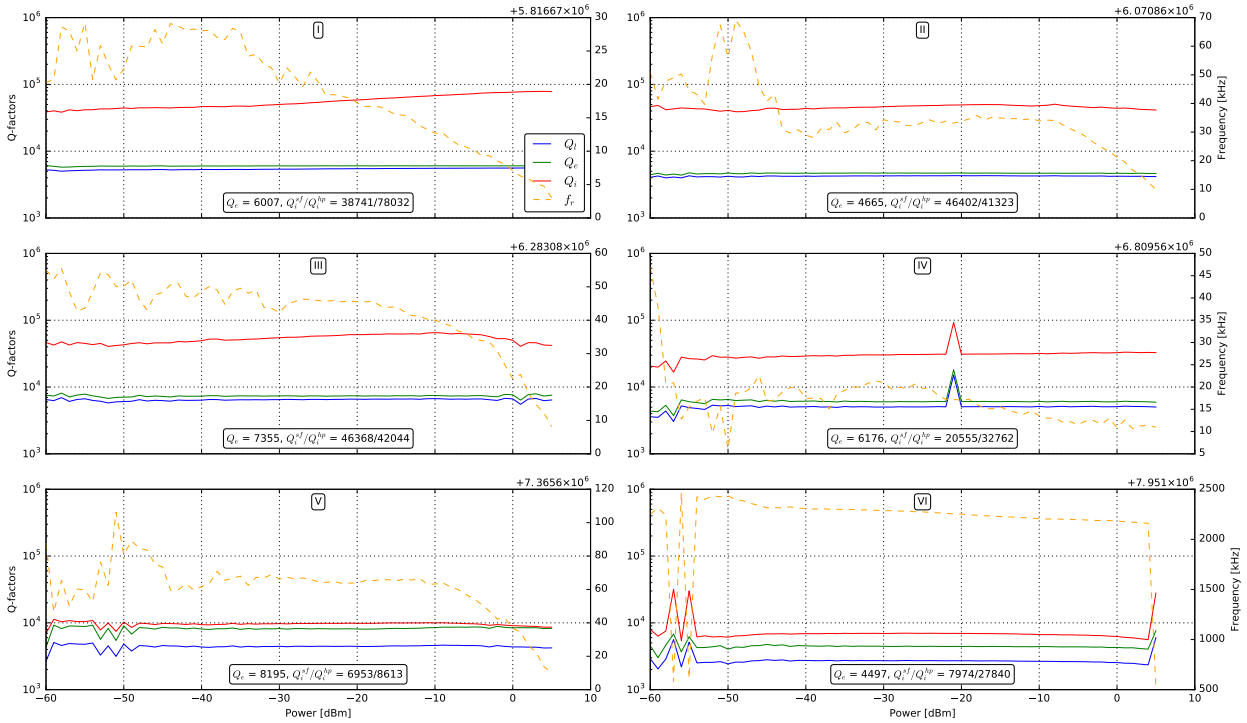

Figure 8.2: Fitting results for the sample.

References

[1] Efficient and robust analysis of complex scattering data under noise in microwave resonators / S Probst, FB Song, PA Bushev et al. // Review of Scientific Instruments. — 2015. — Vol. 86, no. 2. — P. 024706. (referenced on pp. [3 and 5])

[2] Sank Daniel Thomas. Fast, Accurate State Measurement in Superconducting Qubits : Ph. D. thesis : September / Daniel Thomas Sank. — 2014. (referenced on p. [3])

[3] Measurements of permittivity and dielectric loss tangent of high resistivity float zone silicon at microwave frequencies / Jerzy Krupka, Jonathan Breeze, Neil McN Alford et al. // 16th International Conference on Microwaves, Radar and Wireless Communications, MIKON 2006. — 2007. — Vol. 54, no. 11. — P. 3995–4001. (referenced on p. [3])

[4] Improving the coherence time of superconducting coplanar resonators / H Wang, M Hofheinz, J Wenner et al. // Applied Physics Letters. — 2009. — Vol. 95, no. 23. — P. 233508. (referenced on p. [5])